

Submitted to Sixteenth Annual SEMI-THERM conference

Fan Swirl Effects on Cooling Heat Sinks and Electronic Packages

Ernest Thurlow, Eric Prather, and Vivek Mansingh
Applied Thermal Technologies, Inc.

3255 Kifer Road

Santa Clara, CA 95051

Tel: (408)522-8730, Fax: (408)522-8729

Email: thurlow@applied.fluent.com or eric@applied.fluent.com

Abstract

This paper presents fan swirl effects on cooling heat sinks and electronic packages. The case-to-air thermal resistance, q_{ca} , of a power-dissipating device in a duct was compared with and without swirled airflow, for a variety of heat sink configurations. For a given volumetric airflow rate through the duct, power dissipation, and heat sink geometry, the presence of swirl always reduced q_{ca} . Enhanced cooling due to swirl was most evident at low airflow rates and with crosscut heat sink geometries. Swirl effects were observed as far as 15 diameters downstream of the fan. Based on these results, to improve the accuracy of CFD models, the effects of swirl should be taken into account in analysis of heat sinks and packages downstream of fans.

Introduction

Accurate prediction of θ_{ca} without a heat sink is critical in determining the temperatures of electronic components. In many instances this thermal resistance is determined using a uniform flow in a duct [1-2], where $\theta_{ca}=(T_{case}-T_{ambient})/P$, P is the power dissipated, and T is the measured temperature. It has been widely accepted [3-5] that vortex generators or other methods of intensifying local turbulence, improve heat transfer and alter thermal resistance of heat sinks and heat spreaders. Most commercial electronic systems use fans or blowers that cool the heat sinks and electronic packages. These fans have a swirl component of air velocity that may enhance cooling of heat sinks and packages as compared to a uniform flow situation in a duct. This paper intends to provide some insight on the cooling effects of fan “swirl” on heat sinks and electronic packages, and the proximity to which these effects are important.

Experimental Arrangement

Two experimental configurations were used to determine the effect of fan swirl on heat sink performance. One configuration included airflow swirl by utilizing a ducted fan upstream of a power dissipating heat sink. In the other configuration, the fan was replaced with its fan frame without blades, while the flow through the fan frame was supplied by a wind tunnel. In this case, no fan swirl was present in the uniform ducted airflow. The results of the two configurations were compared for several airflow rates, different heat sinks, and different

spacing between the fan and heat sinks. The experimental setups of these three different tests are discussed in greater detail below.

A heated copper block was used to represent the power-dissipating package. It was 25.4mmx25.4mm in cross-section, 12.5mm thick and was embedded in the PlexiglasTM base. The copper block protruded 0.3mm from the base. Electric power was dissipated using a TO220 power transistor attached to the bottom of the copper block. The copper block was insulated from surroundings by fused silica powder. A T-type thermocouple was epoxied to the copper block to measure the block temperature, representing case temperature of an electronic package.

The tests were performed in a Plexiglas duct with a 100mmx100mm cross-section as shown in Figure 1. The upstream end of the duct was connected to a calibrated wind tunnel. The power-dissipating copper block was centered in the bottom wall 500mm downstream of the duct inlet. A heat sink was attached to the top surface of the copper block. The thermal interface material between the copper block and the heat sink was Omegatherm “201” high thermal conductivity epoxy paste. The paste thickness was determined to be 0.4 ± 0.02 mm.

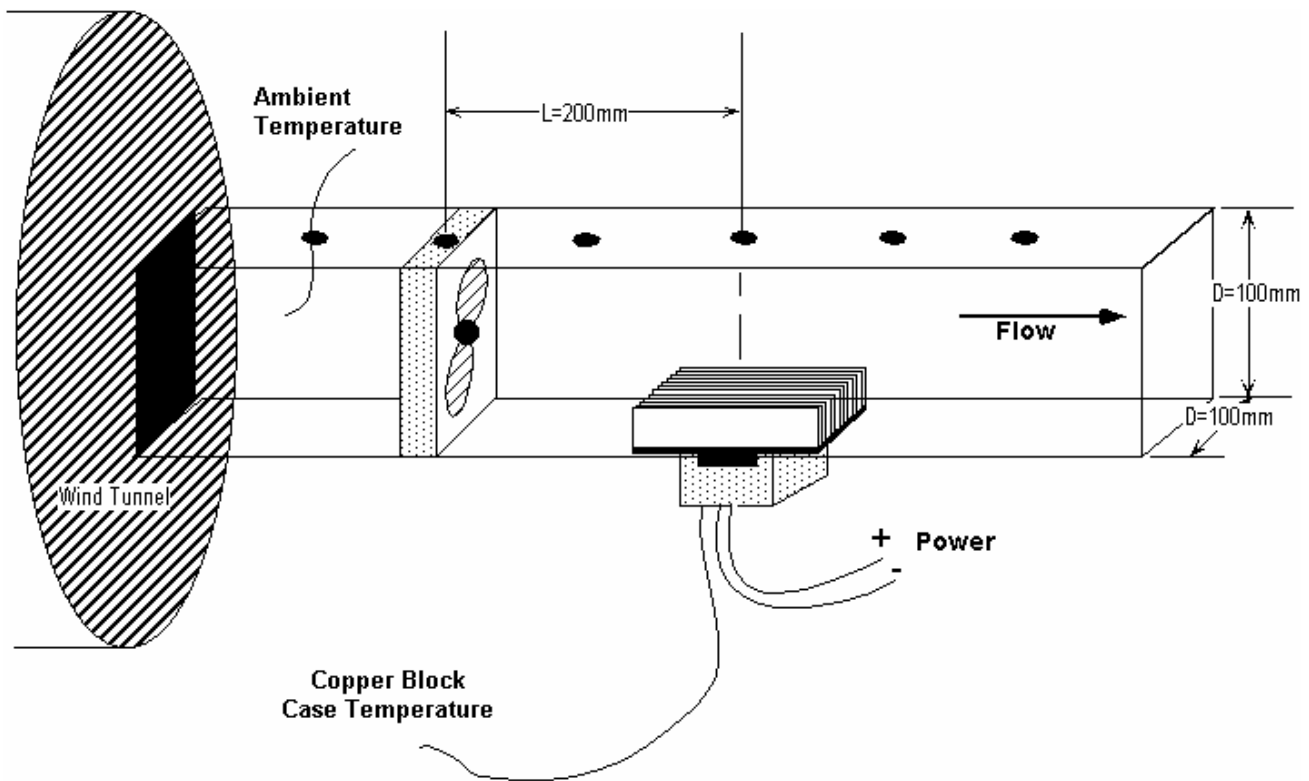


FIG.1. Schematic showing heat sinked copper block embedded in PlexiglasTM channel at $L/D=1$ downstream of fan.

The dimensions of three heat sink types used are listed below in Table 1. Each of the aluminum heat sink surfaces was anodized black. There were two crosscut extruded heat sinks and one extruded fin heat sink that was not crosscut as shown in figures 2a, b, c.

Heat Sink	Aavid #	WidthxLength	Base Thickness	Fin/Pin #	Overall Height	Fin/Pin Thickness
#1, Small Crosscut	373024B	27mmx27mm	1mm	8x8	9mm	1.5mmx2mm
#2, Large Crosscut	372024B	35mmx35mm	2.5mm	7x7	28mm	2mmx3mm
#3, Large Extruded	62200	89mmx76mm	5mm	12	21mm	1.5mm-2.0mm

Table 1. Heat sink dimensions and their Aavid part numbers used in experiment #2.



FIG.2a. Small 89mmx76mmx21mm crosscut extrusion heat sink, #1.

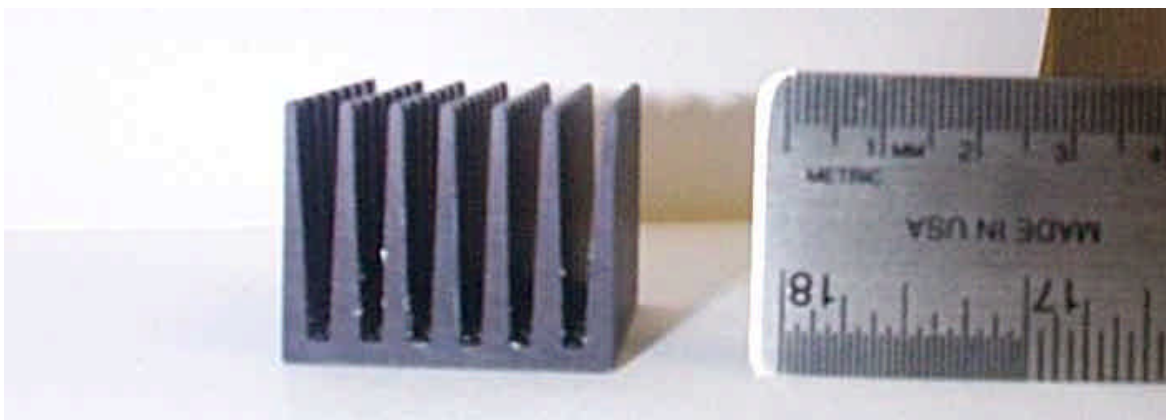


FIG.2b. 1" Tall 35mmx35mmx28mm crosscut extrusion heat sink, #2.



FIG.2c. Large 89mmx76mmx21mm extruded fin heat sink #3.

In one configuration, with the fan operating, the wind tunnel was used to measure the duct airflow rate. In the other configuration, the fan was removed and replaced with its fan frame. The same airflow rate was then supplied by the wind tunnel.

Ambient air temperature was measured at the duct inlet. Both of the temperatures were recorded using a Fluke HydraTM system. The fan used was a Nidec #TA350DC M34138, 92mmx 25mm thick fan with 62CFM free flow. The fan flow curve is shown in Figure 3.

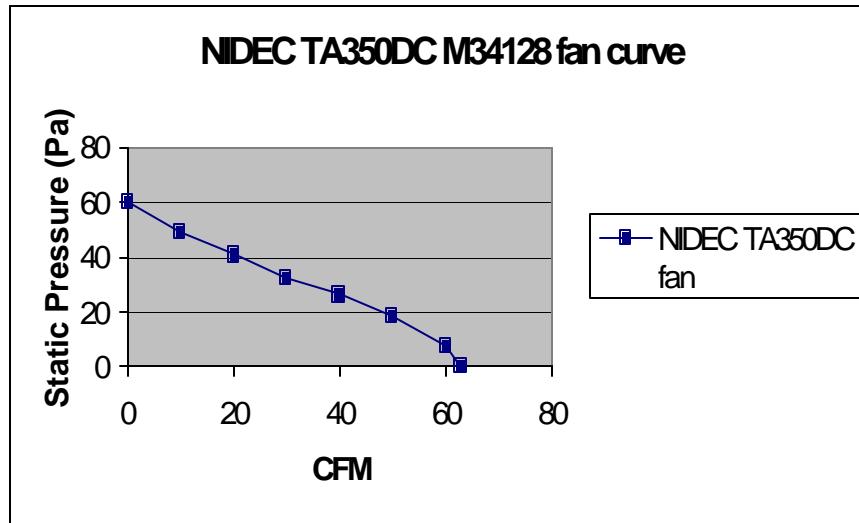


FIG.3. Pressure vs. CFM for NIDEC TA350DC fan used in experiments.

In the first test, the airflow rate and power dissipated in the copper block were varied. Heat sink #3 was attached to the top surface of the copper block, Figure 2c, and the fan was placed at L/D=1 upstream of the copper block, Figure 1. Flow rates were adjusted from 10-40CFM±2% at each power setting, using the wind tunnel to vary the pressure drop across the system. After steady state temperature conditions had been reached, ($dT_{\text{block}}/dt < 0.02\text{C}/\text{min}$), the ambient temperature and the copper block temperature were recorded. These measurements were made for flow with and without fan swirl. 5, 10, 15, 20, and 30W were

dissipated from the heat-sinked copper block for duct airflow rates of 10, 20, 30, and 40CFM.

For the second test, The heat sink geometry and power dissipation were varied. The fan was placed at an $L/D=1$ from the copper block and the airflow was set at 20CFM. θ_{ca} was measured for the three different heat sinks #1, #2, and #3 and without a heat sink. The power settings without a heat sink and the small crosscut heat sink configuration were $P=1,2,3,4W$ and $P=2,4,8,12W$ respectively; while for the large crosscut and large extruded heat sinks the power settings were $P=10,15,20$, and $30W$.

The third test involved varying the spacing between the fan and heat sink. The spacing was varied from $L/D=1$ to $L/D=20$. A constant 20CFM and 30W power input was maintained while the ambient and copper block temperatures were again recorded for the #3 heat sink.

Several of these tests were repeated and results showed repeatability to within $\pm 5\%$.

Experimental Results

For the first test, temperature rises were measured and thermal resistances, θ_{ca} , were calculated for each power and CFM setting, where ΔT_{ca} is the temperature difference measured between the inlet ambient and the copper block surface. Figure 4 shows the effect of fan swirl on package thermal resistance. The results are presented in the form of the package thermal resistance with swirl normalized by the package thermal resistance without swirl, or $\theta_{ca}(\text{fan})/\theta_{ca}(\text{no fan})$, for each configuration.

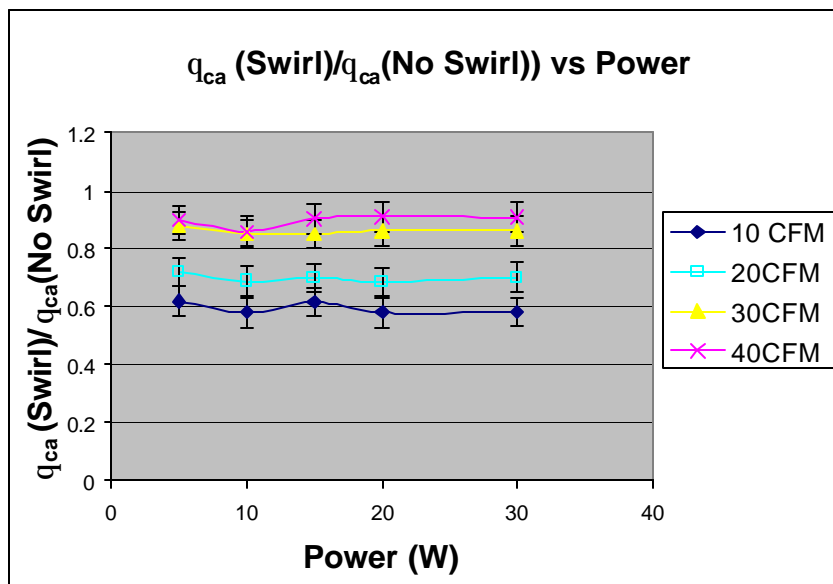


FIG.4. Thermal resistance ratios of swirl measurements to no swirl measurements for copper block subjected to different airflow rates and different power dissipation settings.

As can be seen, with a fan swirl, the increased local velocity near the heat sink surface and the disruption of the boundary layer clearly improves cooling especially at low airflow rates. At 10CFM the thermal resistance reduces by almost 50% in the presence of swirl. The cooling improvement achieved in the presence of fan swirl is a strong function of total airflow rate through the system. At the higher airflow speeds the swirl component of velocity has less effect on cooling a component. Only about a 5-10% reduction in temperature rise occurs at 40CFM.

The variation in thermal resistance for different heat sink types is also noticeable when fan swirl is present, especially when comparing crosscut and extruded heat sinks, Figure 5. Both the large and small crosscut heat sinks significantly improve in performance with swirl present. The large extruded heat sink does not take advantage of fan swirl as well as the crosscut extrusion heat sinks, but still provides a reduction in θ_{ca} with fan swirl

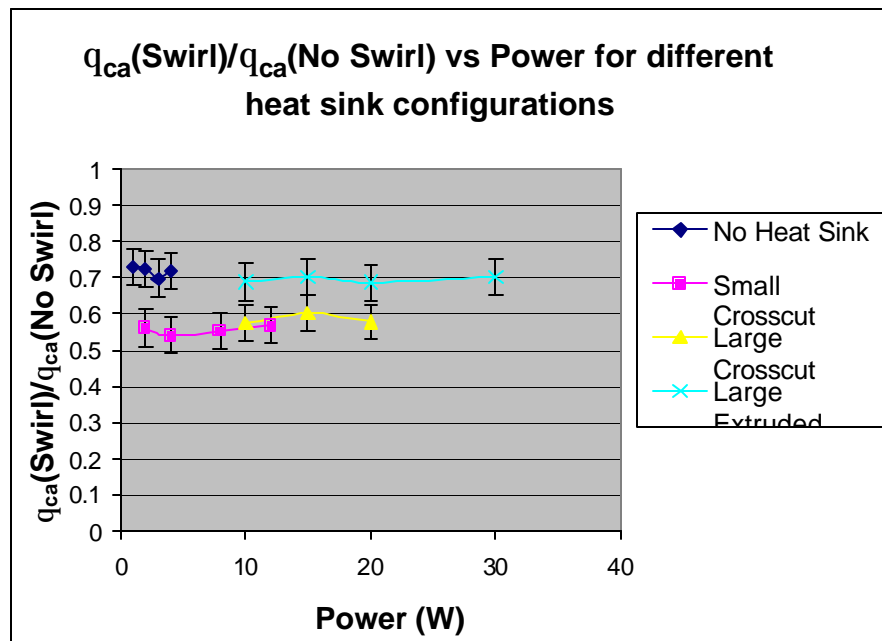


FIG.5. Thermal resistance ratios of swirl measurements to no swirl measurements for three different heat sinks and a without a heat sink.

As mentioned earlier, the third test was conducted to determine how far downstream the effects of fan swirl persist. The effect of distance between the fan and heat sink is shown in Figure 6. The noticeable benefits of the fan exist out to about $L/D=15$ in this duct configuration. At $L/D=15$, where $\theta_{ca_swirl}/\theta_{ca_no_swirl}\approx 0.95$, i.e. a ~5% reduction in temperatures could still be seen using a fan. It seems that all heat sinks should perform relatively better at all L/D with fan swirl present.

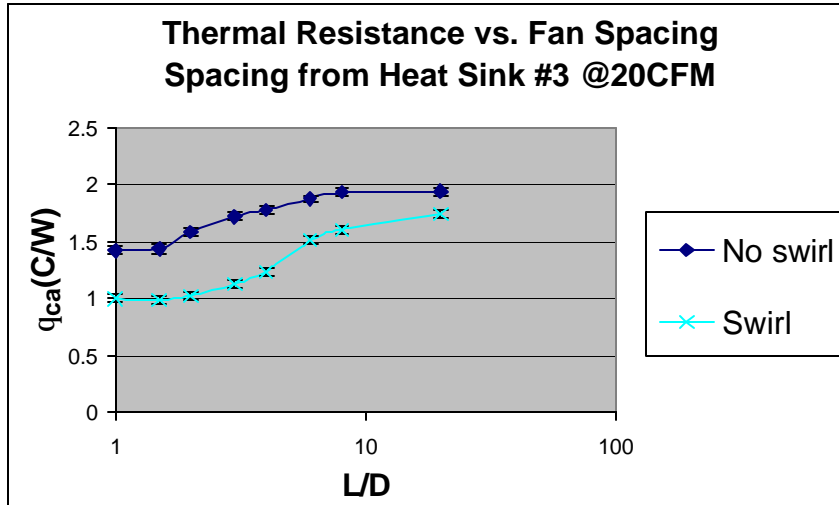


FIG.6. Thermal resistance between copper block and ambient vs. distance between fan/fan frame and copper block with and without fan swirl.

Conclusions

Several tests have been conducted to determine the effect of the fan swirl cooling on heat sinks and electronic packages. It is clearly evident that airflow with an additional fan swirl component, as opposed to a purely uniform airflow, is beneficial to cooling. The effect of swirl persists far downstream of the fan ($L/D > 15$). Crosscut heat sinks definitely take better advantage of this swirl component than a flat plate or extruded heat sinks.

These results show that fan swirl must be considered when attempting to accurately predict temperatures of components downstream of a fan. Further work will be done to quantify swirl effects so CFD analyses can accurately account for fan swirl.

Nomenclature

- L** Streamwise length between fan frame and copper block center
- D** Duct Height and Width=100mm
- D_h** Duct hydraulic diameter, $D_h = 4A/P$
- U** Average duct velocity
- P** Copper block dissipated power
- n** kinematic viscosity of air, $2 \times 10^{-5} \text{ m}^2/\text{sec}^2$
- q_{ca}** Measured thermal resistance between copper block and ambient air
- q_{sa}** Measured thermal resistance between heat sink and ambient air
- DT_{sa,ca}** Measured temperature difference between heat sink base **s**, or copper block surface **c**, and inlet ambient air **a**.
- t** time

References

1. Chu, H.W., Belady, C.L., and Patel, C.D., "A survey of high-performance, high aspect ratio, air cooled heat sinks", *ISPS 1999 Proceedings*, 35, No. 4, pp. 71-76, 1999.
2. Mansingh, V., Kazuhiro, N., Shidore, S., and Addison, S., "Heat sinks for high power multichip modules", *Proceedings of the 1996 IEPS Technical Conference*, pp. 410-421, October 1996.
3. G. Biswas and H. Chattopadhyay, "Heat Transfer in a channel with built-in wing-type vortex generators", *Int. J. Heat Mass Transfer*, 35, No. 4, pp. 803-814, 1992.
4. P.A. Eibeck and J.K.Eaton, "Heat transfer of a longitudinal vortex embedded in a turbulent boundary layer", *J. Heat Transfer*, **109**, pp. 16-24, 1987.
5. F.J. Edwards and G.J.R. Alker, "The improvement of forced convection surface heat transfer using surface protrusions in the form of (a) and (b) vortex generators", *Proc. Fifth Int. Heat Transfer Conf., Tokyo*, **2**, pp. 2244-2248, 1974.